COBEM 2021 26th International Congress of Mechanical Engineering
November 22-26, 2021, Virtual Congress, Brazil
ABCM Associação Brasileira de Engenharia e Ciências Mecânicas

COBEM2021-2120 Structural analysis of the nose clip from the antiviral filtering facepiece respirator N95 - VESTA

Matheus Filippe S. Alves
Caio C. Abreu Bílio
Léo Diniz Czarnewski
Braion B. Moura
Marcela R. Machado
Department of Mechanical Engineering, University of Brasília,Campus Universitário Darcy Ribeiro, Faculdade de Tecnologia - Asa Norte, Brasília - DF, 70910-900
marcelam@unb.br

Abstract. *The pandemic caused by the coronavirus (SARS-CoV-2), which causes the disease COVID-19, forced health authorities and research institutes to propose solutions. An important and accessible tool to fight against the virus the use of masks. The VESTA respirator's designed product is the new antiviral N95 filtering facepiece respirator developed by the researcher team from the University of Brasilia. The VESTA differential is the chitosan nanofilm, present in the intermediate layer, that works as a physical barrier for the virus. The nanofilm has antimicrobial action and greater ability to filter viruses, including the SARS-CoV-2 that causes COVID-19. The respirator consists of a semi facial piece composed of filtering material covering the nose, mouth and chin. It is fixed on the face by two elastics headband and a nasal clip to reinforce the face's sealing. This paper analyses the VESTA nasal clip structural characteristic as tension, deformation, and vibration. This device is responsible for securing the sealing around the user's nose. The nose clip improves the protection of leakage between the respirator and the face. Numerical simulation of the nasal clip structural analysis was performed using ANSYS.*

Keywords:*Finite element method, Structural analysis, N95 filtering facepiece respirator, Nose clip, COVID-19.*

1. INTRODUCTION

The speed of dissemination of COVID-19 led to an alert to the World Health Organization (WHO), which classified the emerging disease as a pandemic, characterised by a global health problem of an emergency nature (Shereen *et al.*, 2020). The growing demand for personal protection equipment (PPE) and its scarcity for health professionals and society motivated researchers to develop PPE more efficiently to maintain its quality and low-cost production. A multidisciplinary research team from the University of Brasília developed a facepiece respirator-class N95 able to filter nanoparticles and inactivate the virus, such as the SARS-CoV2 virus, bringing users a safer environment. The adoption of emergency measures is necessary given the continuous increase in new SARS-CoV mutations. Measures to prevent the massive spread and worsen the country's disease have taken the Brazilian health system to the limit of its capacity. Besides vaccines, it is essential to use masks, respirators, and constant hand hygiene. Healthcare professionals are highly exposed to SARS-CoV-2 because of the high demand from healthcare systems to deal with the pandemic. There is a consensus among public health agencies to adopt protective measures related to the use of PPE, such as face shields and semi-facial respirators with N95 particle filters, to reduce airborne disease transmission (NIOSH, 2015).

VESTA is the new N95 class antiviral filter respirator developed by a team of researchers at the University of Brasília. This respirator is a facepiece composed of three layers of nonwoven fabrics (TNT-dental-hospital) capable of retaining up to 95% of solid, liquid, oil and aerosol particles. The differential of the Vesta Respirator is the chitosan nanofilm present in the mask's intermediate layer. Besides working as a physical barrier against the virus, it is also a barrier that, through chemical interaction, has the property of inactivating the virus. In addition, nanofilm has antimicrobial action and greater ability to filter viruses, including SARS-CoV-2. The nanofilm is produced from chitosan nanoparticles, a cationic polymer - a natural macromolecule - found in shrimp shells. The chitosan material is low-cost, biodegradable, biocompatible, non-toxic, and possesses properties able to inactivate the virus. Therefore, this PPE improves protection against contamination and reduces SARS-CoV-2 infection in healthcare professionals working in hospitals and the general population.

A facepiece respirator protects its wearer by sealing its face and filtering out hazardous particles from the environment. However, it is common for the face seal leakages of users. Therefore, a numerical model has been performed to simulate the use of the respirator and help improve its design. Zhipeng et a.l. (Zhipeng *et al.*, 2012) have investigated headform and N95 filtering facepiece respirator interaction according to the contact pressure through simulation and experimental validation. In the respirator contact, the interactions first happen on the frontal maxilla and the nasal regions. In this work,

the authors carried out structural simulations such as stress, strain and vibration analysis on Vesta's nose clip. This device is responsible for securing the sealing around the user's nose to improve the protection of leakage between the respirator and the face (Zhipeng and James, 2013), as well as particle penetration through the filter medium. The knowledge of the clip's mechanical characteristics is required for the respirator design, improvement of the respirator, and guiding the designers on the project stage. Numerical simulations were performed in commercial finite element software ANSYS.

2. FINITE ELEMENT THEORY BACKGROUND

The finite element method is a numerical tool that uses variational formulations and uses interpolation methods to solve difficult analytical formulation (Petyt, 2010). The concept of the method is to solve a problem of balance where a complex global structure is divided into partitions, called elements. The elements are then connected, where boundary conditions of movement or rotation restriction and loading can be applied. By solving the set employing numerical methods of approximation of result. The finite element formulation is, to begin with, a variational principle related to total potential energy, The form of Hamilton's principle to be used is therefore

$$\int_{t_1}^{t_2} \left(\delta\left(T-U\right)+\delta W_{nc}\right)+dt=0, \tag{1}$$

There are several techniques for determining approximate solutions to Hamilton's principle. One of the most used methods is the Rayleigh-Ritz, known as the finite element displacement method. The element model is shown in Fig. 1, the generalized coordinates at each node are v, the total deflection and θ, the total slope. This results in an element with four degrees of freedom, two-node element with two-DoF at each node, i and j are local node numbers.

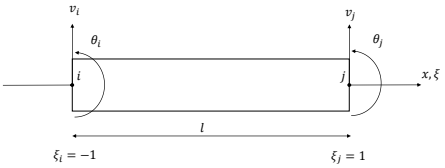

Figure 1. Beam Element.

By using the local coordinate (ξ) and element length l defined in Fig. 1, the displacement v can be written in matrix form as follows $v\left(\xi\right)=\left[\mathbf{N}\left(\xi\right)\right]\left\{\mathbf{v_e}\right\}$ where $\mathbf{N}$ is a shape function of the form,

$$\left[\mathbf{N}\left(\xi\right)\right]=\left[\mathbf{N_1}\left(\xi\right)\mathbf{aN_2}\left(\xi\right)\mathbf{N_3}\left(\xi\right)\mathbf{aN_4}\left(\xi\right)\right], \tag{2}$$

The energy functions for beam are given by

$$T=\frac{1}{2}\int_0^l \rho A\dot{v}^2 dx, \qquad U=\frac{1}{2}\int_{-1}^{+l} EI\left(\frac{\partial^2 v}{\partial x^2}\right)^2 dx, \tag{3}$$

Substituting the displacement into the kinetic energy Eq. (3)

$$T=\frac{1}{2}\int_{-1}^{+1} \rho A\dot{v}^2\left(\xi\right)ad\xi=\frac{1}{2}\left\{\dot{\mathbf{v}}_\mathbf{e}\right\}^T\left(\rho Aa\int_{-1}^{+1}\left[\mathbf{N}\left(\xi\right)\right]^T\left[\mathbf{N}\left(\xi\right)\right]d\xi\right)\left\{\dot{\mathbf{v}}_\mathbf{e}\right\}, \tag{4}$$

such that

$$T=\frac{1}{2}\left\{\dot{\mathbf{v}}_\mathbf{e}\right\}^T\left[\mathbf{M_e}\right]\left\{\dot{\mathbf{v}}_\mathbf{e}\right\}, \tag{5}$$

where $\dot{\mathbf{v}}_\mathbf{e}$ is the velocity vector of the beam element, $\mathbf{M_e}$ is the mass matrix of the beam element. Substituting the displacement into the strain energy Eq. (3) gives

$$U=\frac{1}{2}\int_{-1}^{+1} EI\frac{1}{a^4}\left(\frac{\partial^2 v\left(\xi\right)}{\partial\xi}\right)^2 ad\xi=\frac{1}{2}\left\{\mathbf{v}_e\right\}^T\left(\frac{EI}{a^3}\int_{-1}^{+1}\left[\mathbf{N}''\left(\xi\right)\right]^T\left[\mathbf{N}''\left(\xi\right)\right]d\xi\right)\left\{\dot{\mathbf{v}}_\mathbf{e}\right\}, \tag{6}$$

such that

$$U=\frac{1}{2}\left\{\dot{\mathbf{v}}_\mathbf{e}\right\}^T\left[\mathbf{K_e}\right]\left\{\dot{\mathbf{v}}_\mathbf{e}\right\}, \tag{7}$$

For the analysis of a structure, ANSYS may be broken into the following three stages (Stolarski *et al.*, 2006): Pre-processing, processing and Postprocessing. In particular, model generation (element type, mesh and material/geometric

properties) or defining the problem is done in the Preprocessor and application of loads, constraints and the solution is performed in the Solution Processor. This is used for obtaining the solution for the finite element model that is generated within the Preprocessor. Finally, the results are viewed in the Postprocessor. This includes the plotting of contours, deformed shapes, vector displays, and listings of the results.

Modal analysis is used to calculate the natural frequencies and vibration modes of a structure, which are important design parameters for loading conditions. It also can be a starting point for another, more detailed, dynamic analysis, such as transient dynamic analysis, a harmonic response analysis, or a spectrum analysis (Altabey *et al.*, 2018). There are different modes extraction methods, such as Block Lanczos, PCG Lanczos, Subspace, Supernode, Reduction (Householder) damped and QR damped (ANSYS, 2009). In this work, the Block Lanczos mode extraction was used, an acceptable eigenvalue extraction method for problems with a high number of nodes and for presenting a good convergence rate when applied to problems with symmetric matrices.

Harmonic analysis is used to determine the response of a structure to time-varying cyclic loads. Therefore, it gives the ability to predict the sustained dynamic behaviour of structures, thus verifying whether or not the designs will successfully overcome resonance, fatigue, and other harmful effects of forced vibrations. Analyses can generate plots of displacement amplitudes at given points in the structure as a function of forcing frequency.

3. PRODUCT INFORMATION

The VESTA is a new antiviral N95 filtering facepiece respirator class PFF-2 N95 contend an antiviral nanofilm. The differential of Vesta is the chitosan nanofilm, present in the intermediate layer, which in addition to serving as a physical barrier for the virus, is also a barrier that, by chemical interaction, has the property of inactivating the virus as illustrated in Fig. 2. In addition, the nanofilm has antimicrobial action and greater ability to filter viruses, including the SARS-CoV-2 that causes COVID-19. The VESTA filtering facepiece respirator consists of a semi facial piece of filtering material that covers the nose, mouth and chin according to the specification of NBR-13698:2011(ABNT-NBR, 2011). Two rubber straps are fixed on the face, and the nose clip reinforces the face sealing to guarantee frontal adjustment.

The new antiviral N95 filtering facepiece respirator comprises three layers of nonwovens fabric that can retain up to 95 % of solid, liquid, oily and aerosol particles. The middle layer is the filtering element containing the nanotechnology, the chitosan nanofilm, which is the differential of Vesta. Nanotechnology works as a physical barrier for the virus, and by chemical interaction, it has the property of inactivating the virus. In addition, the nanofilm has antimicrobial action and greater ability to filter viruses, including the SARS-CoV-2 that causes COVID-19. The nanofilm is produced from chitosan nanoparticles, a cationic polymer - a natural macromolecule - found in the shrimp shell. Chitosan material is biodegradable, biocompatible, non-toxic and has properties to inactivate the virus. In addition, it is a low-cost material.

Figure 2. Illustration of the new antiviral N95 filtering facepiece respirator- Vesta

VESTA design (Rosa *et al.*, 2020) follows the ANVISA resolution RDC N 356/2020 (ANVISA, 2020) recommendations establishing that the N95 filtering facepiece respirator should have the finishing of the pieces free of burrs and sharp. The manufacturing material of VESTA is the nonwoven fabric for odonto-medical-hospital use, the performance of surgical mask (ABNT-NBR, 2004). The technology developed and applied to the filter layer is based on chitosan nanoparticles that aim to reduce SARS-CoV-2 contamination and infection among users. This application would enhance the filtering power of the respirator, aiming to mitigate the harmful effects of bacteria and viruses, especially in the hospital environment. Chitosan is a low cost natural cationic polymer derived from chitin, with a biodegradable, biocompatible, non-toxic characteristic, in addition to its antimicrobial activity. Virucidal activity is based on the attractive factor of its cationic charge for negative charges, as is the case with viruses. Thus, chitosan can act as a surface for adsorption and viral inactivation. The use of nanomaterials in facial respirators can decrease the permeability of particles and promote an

effective antiviral effect compared to conventional respirators such as N95.

3.1 Nose clip design

The 3-D model of the nose clip was performed in SolidWorks and the computer-aided engineering(CAE) simulation in ANSYS. Figure 3 (a) shows the Vesta nose clip composed of a composite material filled with a PVC (Polyvinyl chloride) matrix and reinforced by two aluminium alloy wires, and Fig.3 (b) its computer-aided design (CAD) model. The

(a) (b)

Figure 3. Vesta nose clip made of rigid PVC (a), and VESTA mask's nose clip design(b).

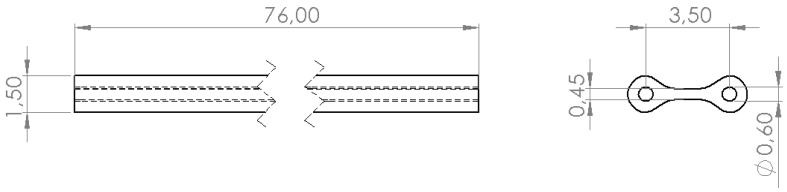

Figure 4. Nose clip dimensions [mm].

composite matrix is responsible for fixing the fiber reinforcement and shaping the composite component. On the other hand, the functions of the reinforcement in a composite material are to increase the composite's mechanical properties and provide strength and stiffness to the composite in one direction as reinforcement carries the load along the length of the fiber. Figure 4 shows its general dimensions and shape according to the supplier's datasheet.

Composite materials can be defined as a material structure consisting of two or more macroscopically identifiable materials working together to accomplish a superior result (Thomas *et al.*, 2012). For instance, the VESTA nose clip structure is produced from a polymer matrix made with Rigid PVC and a metal reinforcement mechanism using two wires made with Aluminum Alloy 1350-H19. The PVC is a high-strength thermoplastic material widely used in several applications such as pipes, medical devices, wire, and cable insulation. Due to the PVC versatile properties, such as lightweight, durable, low cost and easy processability, it has been replacing traditional building materials like wood, metal, concrete, rubber, ceramics, etc. VESTA's nose clip is manufactured with unplasticized or rigid PVC, also known as UPVC (PVC-U or uPVC). It is a stiff and cost-effective thermoplastic polymer with high resistance to impact, water, weather, chemicals and corrosive environments. Kalaga and Neelam (Kalaga and Neelam, 2002) described that plastics are anisotropic material with high nonlinearity. The typical nonlinearity exhibited during the pre-yield stages of tensile loading. Nevertheless, by considering that this paper is only evaluated the pre-yield stages of tensile loading for the nose clip reinforcement, an approximation is made to the mechanical behaviour of the PVC matrix, considering it linear, simplifying the proposed analysis.

The Aluminium Alloy 1350 is a high (99.5% min.) aluminium-content alloy with small additions of silicon, iron, copper, manganese, and other elements. Alloy 1350 is highly conductive and has good formability, leading to its use in electronics and other applications. It is available in various forms such as powder, bar, ingot, ribbon, wire, shot, sheet, and foil. Linear Formula: Al / Fe 0.40% / Si 0.10% / Cu 0.05% / Zn 0.05% / Mn 0.01% / Cr 0.01%. Aluminum Alloy 1350-H19 is 1350 aluminium in the H19 temper. By achieving this temper, the metal is strain hardened to a strength that exceeds H18 by at least 10 MPa. It has the second-highest strength and lowest ductility compared to the other variants of 1350 aluminium. Table 1 shows the material mechanical properties required to solve the static analysis using Rigid PVC (Callister, 2000) and Aluminum Alloy 1350-H19 (MatWeb, 2021).

Table 1. Mechanical Properties of the Rigid PVC and Aluminum Alloy 1350-H19.

Properties	**Rigid PVC**	**Aluminum Alloy 1350-H19**
Density, kg/m^3	1440	2705
Young's Modulus, GPa	3.25	69
Poisson's Ratio, MPa	0.38	0.33
Tensile Yield Strength, MPa	42.75	165
Compressive Yield Strength, MPa	42.75	165
Tensile Ultimate Strength, MPa	46.2	186
Compressive Ultimate Strength, MPa	0	0

Mechanical properties for fatigue analysis

The evaluation of fatigue conditions requires knowing the material behaviour when applying a cyclic loading. Hence, an SN-Curve (sometimes written S-N Curve) is a plot of the magnitude of alternating stress versus the number of cycles to failure for a given material. The fatigue testing of polymers has revealed significant differences between the fatigue response of polymers and metals (Dao and Dicken, 1987). Generally, fatigue failure in metals is a process of crack initiation, propagation, and failure. Fatigue damage in metals is cumulative and cycle-dependent but remains essentially independent of test frequency. The fatigue behaviour of polymers is influenced by viscoelastic effects, unlike of metals. At high frequencies, softening and melting occur, and fatigue failure depends largely on the test frequency. At lower frequencies, fatigue failure becomes less sensitive to test frequency and results from crack initiation and propagation. Based on the experimental works of Alexander and Potter(Alexander and Potter, 2014) and Almeida (De Almeida, 2018) the SN-Curves for the rigid PVC is showed in Fig. 5(b) and for the Aluminum Alloy 1350-H19 in Fig. 5(c).

(a)

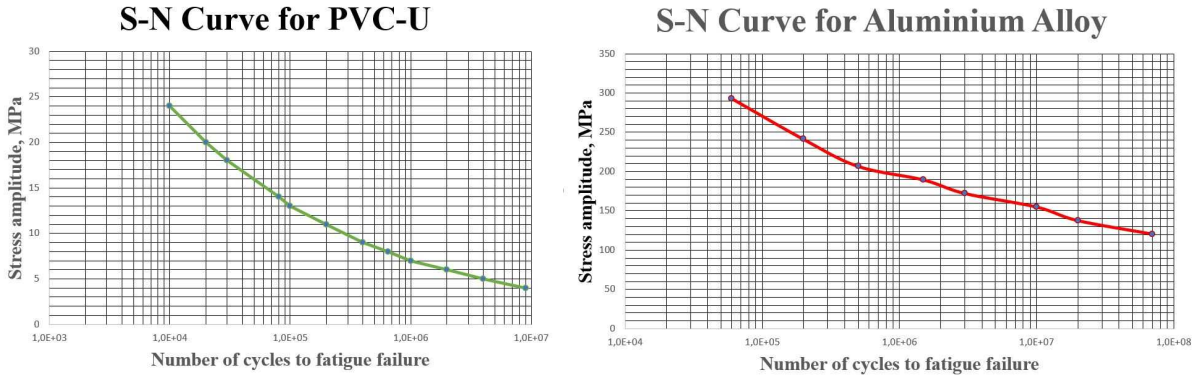

(b) (c)

Figure 5. Aluminum 1350-H19 wires(a);S-N Curve for Rigid PVC(b);S-N Curve for Aluminium Alloy(c).

In general, alloys made of non-ferrous materials, like Aluminum Alloy 1350-H19, have a behaviour that has no asymptote in S-N Curves.

4. STATIC ANALYSIS RESULTS

This section shows the tension, torsion, bending, and fatigue analysis performed for the nose clip. The objective is to evaluate the limit values for each loading type in the pre-yield stages. For the fatigue analysis, it is expected to evaluate the fatigue life under bending. In bending analysis, a support is used to simulate the contact between nose and nose clip as

in real situations. The same strategy is used to analyse the fatigue life. The nose clip strength can be compared according to the Normative Data of Grip and Pinch Strengths in Healthy Adults presented in (Mohammadian *et al.*, 2014), where mean tip pinch strength is defined by 8.8 kg and mean palmar pinch strengths is 10.3 kg for the dominant hand of men. Figure 6 is an example of pinch types. in this paper, one has a focus on analyses maximum limit of work applied to the nose clip. The nose clip is a piece selected, and the manufacturer does not give such information to the designers. The structural analyses presented in the following sections will help understand the limits of the VESTA's nose clip.

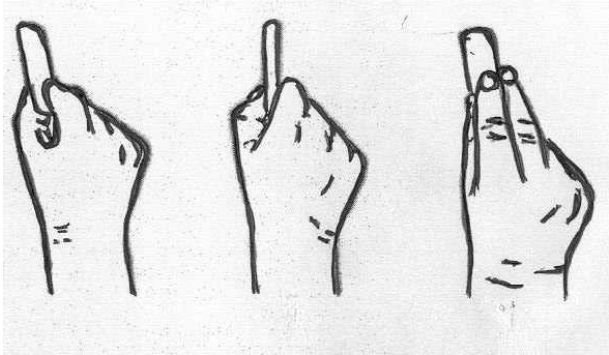

Figure 6. Illustration of the three kinds of pinch: tip, lateral and palmer respectively from left to right (Mohammadian *et al.*, 2014).

Static analysis was performed by using the commercial finite element method ANSYS-Workbench. Figure 7(LHS) shows the meshing clip for the tension and torsion analysis, and Fig 7(LHS) for the bending and fatigue, which included the clip and the support simulation of the nose. Table 2 gives each analysis the number of elements and nodes in the mesh. In all cases, we used the SOLID186 ANSYS elements in the mesh. The elements close to the boundary conditions and load application regions were carefully disregarded in the stress analysis.

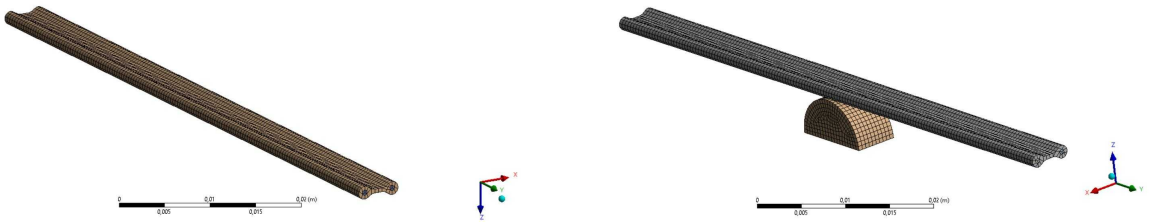

Figure 7. Meshing 1 - Tension and Torsion (LHS) and Meshing 2 - Bending and Fatigue (RHS)

Table 2. Number of elements and nodes in the mesh in each analysis.

Analysis	**Elements**	**Nodes**
Tension and Torsion	4408	29474
Bending and Fatigue	6196	37110

Tension analysis

The application of boundary conditions and load consists of constraints in a certain degree of freedom and indicates that the load will act in each degree of freedom. A tensile load of 92.4 N was applied on the clip's end, denoted B for the tension analysis. It assumed a fixed-free boundary condition with the contained edge in point A, as indicated in Fig. 8. Figure 9 shows the equivalent von Mises stress for the tension of the clip. The composite reinforcement absorbs the highest stress values, keeping the matrix region in the pre-yield stage. The maximum equivalent von Mises stress is about 162 MPa in the aluminium wires and 20 MPa in the PVC body of the clip. For reliable usage, the maximum stress limit should be considered at 20 MPa because otherwise, the aluminium wires would enter in a non-linear zone leading to crack nucleation. Figure 10 shows the safety factor for tension, which is the ratio between the strength of the material and the maximum stress in part. When the stress in a specific position becomes superior to the strength of the material, the safety factor ratio becomes inferior to 1 when there is a risk, and it must be avoided. The clip under specified tensile load presented a safety factor of 5 for the PCV and 0.97 to the aluminium wire, demonstrating the limitations of the force applied on the clip.

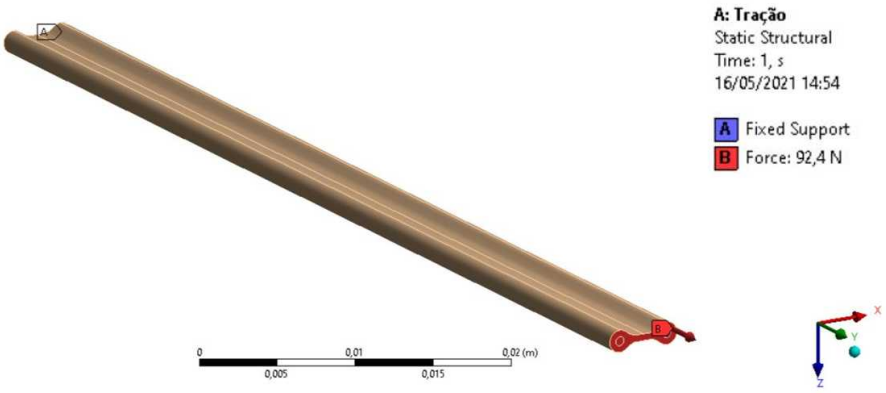

Figure 8. Nose Clip under tension.

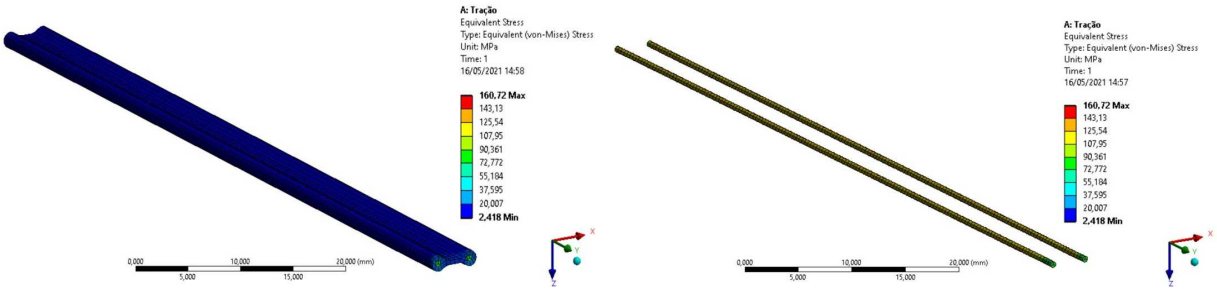

Figure 9. Equivalent von Mises stress for tension.

Figure 10. Safety Factor for tension.

Torsion analysis

Torsion loading represented by a moment of 11.43 Nmm is applied on clip's edge A of the, and constrains assumed on edge B, as illustrated in Fig. 11. Unlike tension analysis, Equivalent von Mises stress for torsion shows that the composite reinforcement does not absorb the highest stress values. In this case, the matrix region is responsible for supporting the torque applied, keeping the nose clip in the pre-yield stage. The maximum equivalent von Mises stress is about 44 MPa in the PVC matrix and 5 MPa in reinforcement, see Fig. 12. The PVC matrix would enter in the non-linear zone around 11.43 Nmm torque. The minimum safety factor was 5.62, as shown in Fig. 13.

Bending and fatigue analysis

For bending and fatigue analysis, a bending moment of 16.5 Nmm is imposed on the clip's edge A and B, and fixed support is assumed on surface C. The composite reinforcement supports the highest stress values, keeping the matrix region in the pre-yield stage for bending analyses. The maximum equivalent von Mises stress is about 157 MPa in the aluminium wires and 35 MPa in the PVC body of the clip, shown in Fig. 15. The bending moment of the PVC matrix would enter in a non-linear zone above 16.5 Nmm and the minimum safety factor was 1.04, as presented in Fig.16.

Table 3 shows a comparison of the loads used in tension, torsion, and bending analysis related to the pinch strengths of the adult male hands (MPSAMH). By using the same value of bending moment as a cyclic loading of 16.5 Nmm, Fig 17 gives the number of cycles according to the material. For instance, the PVC matrix-supported around 70 cycles, and for the aluminium reinforcement around 10^7 cycles.

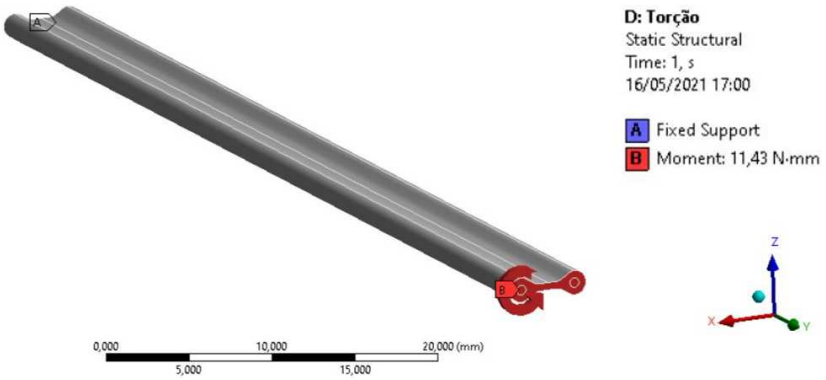

Figure 11. Nose Clip under torsion force.

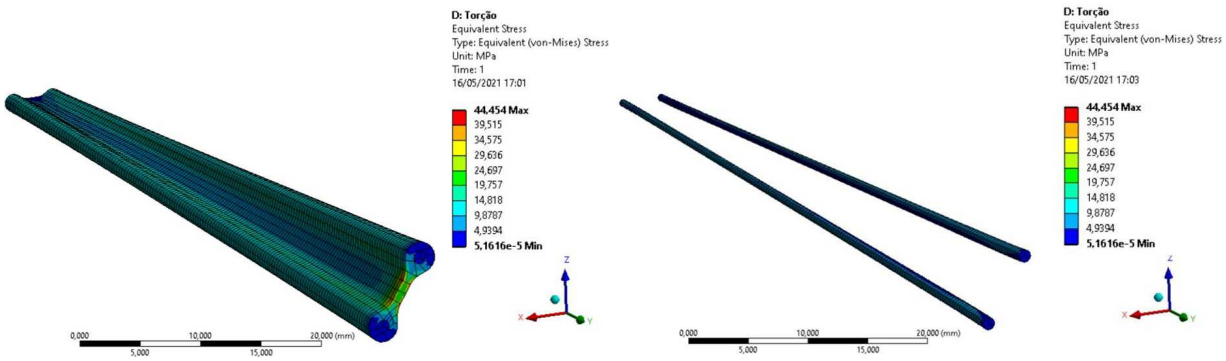

Figure 12. Equivalent von Mises stress for torsion.

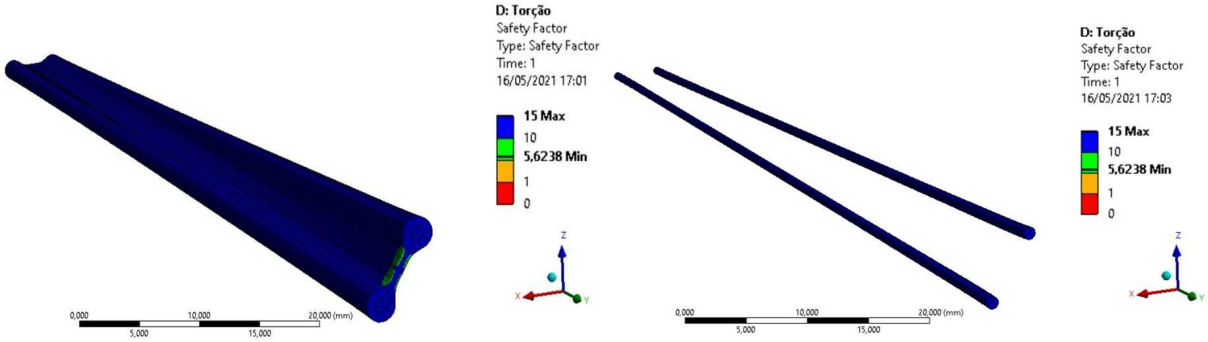

Figure 13. Safety Factor for tension.

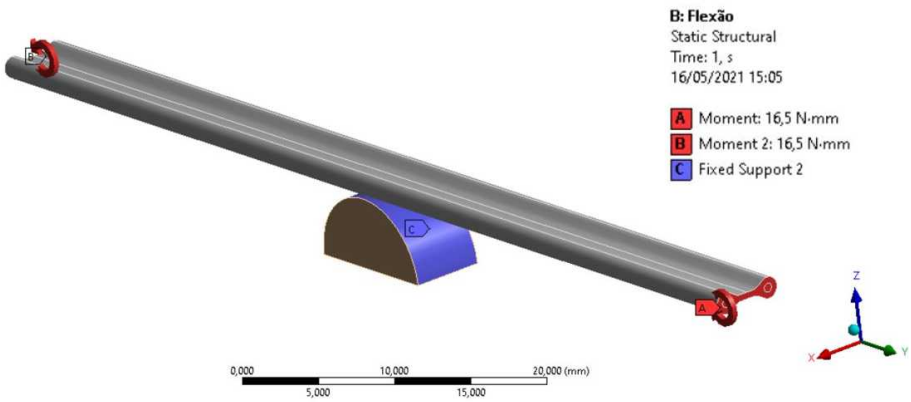

Figure 14. Nose Clip under bending.

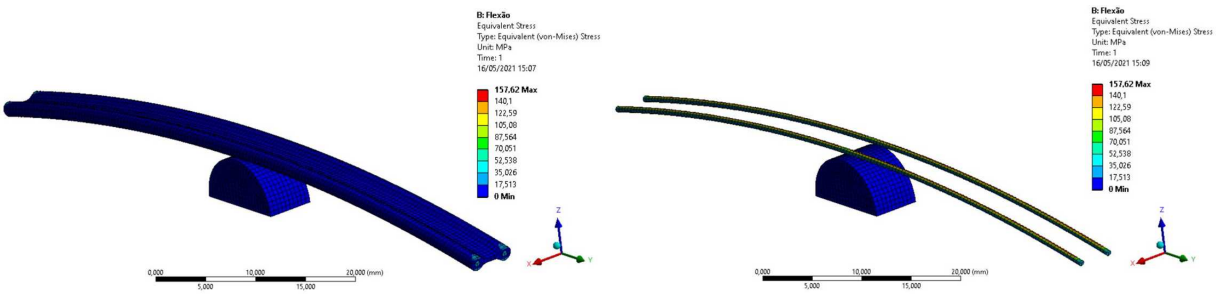

Figure 15. Equivalent von Mises stress for bending.

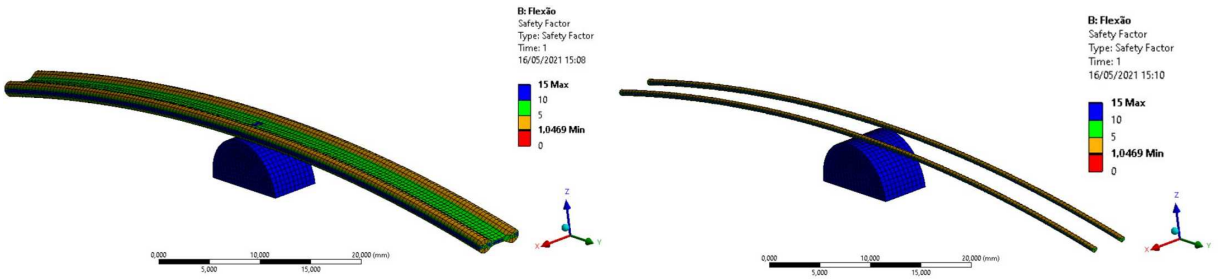

Figure 16. Safety Factor for tension.

Table 3. Percentage of load supported by the clip compared to human manual force.

Analysis	**Loading**	MPSAMH	**%**
Tension	92.4 N	101 N	91.5%
Torsion	11.4 Nmm	431,5 Nmm	2.6%
Bending	16.5 Nmm	6558.8 Nmm	0.25%

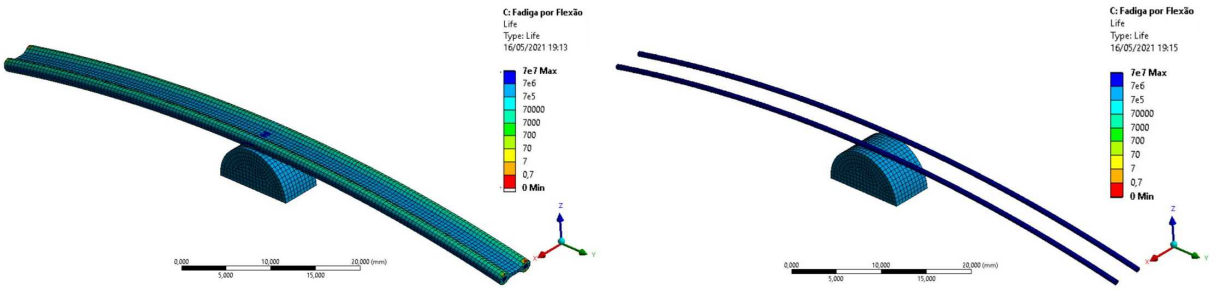

Figure 17. Life - Fatigue Analysis.

5. RESULTS OF DYNAMIC ANALYSIS

The dynamic analysis explored the modal parameters (natural frequencies and modal shape) of the nose clip. One assumed a free-free boundary condition. Clip materials were described in Table1. A mesh convergence analysis to decrease the computation cost assumed a mesh containing 4256, 546, and 288 elements.

Table 4. Natural Frequencies

Frequency	For 4256 Finite elements [Hz]	For 546 Finite elements [Hz]	For 288 Finite elements [Hz]
1	348	346	350
2	961	954	965
3	1882	1868	1892
4	2048	2060	2065
5	2621	2622	2621
6	3107	3085	3126

The firsts six modes are listed in Table 4 and associated with the number of elements in the mesh. The number of

elements did not show an expressive change in the natural frequencies that oscillated around a mean value. Figure 18(a-f) illustrates the vibrational and natural frequencies obtained in the simulation. We observed four bending modes occurring in the frequencies 346, 954, 1868, and 3107 Hz, also two torsion modes in 2060 and 2622Hz. The first natural frequency and modal shape contribute direct to the fatigue in structures and systems, the knowledge of the vibration characteristic is essential in the design stage.

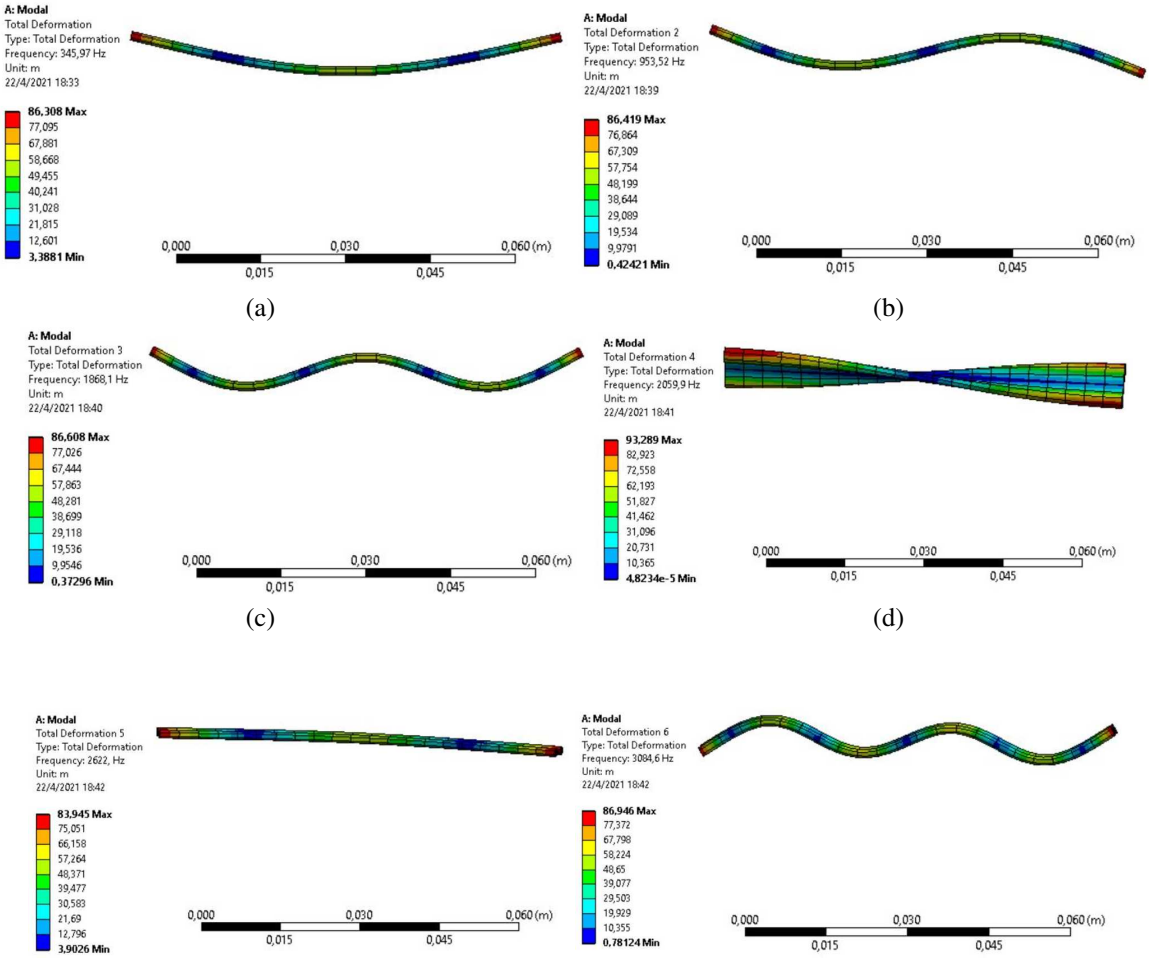

Figure 18. Vesta

6. DISCUSSION AND FINAL REMARKS

This paper presented a computer-aided technique, which combined the FE method and the CAD method to design and assess the respirator VESTA nose clip. The respirator contact happened on the frontal maxilla and the nasal regions, which required the clip device. Mechanical simulation approach tension, bending, fatigue and vibration were performed for the clip. The clip is manufacture with a composite material including PVC and aluminium-alloy wires. The clip maximum tension, torsion, bending, and fatigue was estimated by applying loads based on pinch strengths of the adult male hands (MPSAMH). It is important information that characterizes the component mechanically and demonstrates the limits of the use.

7. ACKNOWLEDGEMENTS

The authors would like to acknowledge the grant received from FAPDF and CNPq through the Programa de Bolsas de Iniciação Científica da Universidade de Brasília(ProIC/DPG/UnB).

8. REFERENCES

ABNT-NBR, 2004. “Nbr 15052-2004- nonwovens - products for odonto-medical-hospital use - performance of surgical mask”. *ASSOCIAÇÃO BRASILEIRA DE NORMAS TÉCNICAS.*, Vol. 13698, No. 2004, pp. 1–24.

ABNT-NBR, 2011. "Nbr 13698-2011 equipamento de proteção respiratória - peça semifacial filtrante para partículas. rio de janeiro, 2011". *ASSOCIAÇÃO BRASILEIRA DE NORMAS TÉCNICAS.*, Vol. 13698, No. 2011, pp. 1–24.

Alexander, N.A. and Potter, R., 2014. "Increasing the lifetime of ferrule strap connections on pvc-u pipes: A study based on theoretical and experimental evidences". In *9th International conference on Civil and Structural Engineering Computing*. The Netherlands.

Altabey, W., Mohammad, N. and Libin, W., 2018. *Using ANSYS for Finite Element Analysis, Volume I: A Tutorial for Engineers*, Vol. I.

ANSYS, 2009. "Theory reference for the mechanical apdl and mechanical application". www.anays.com. Accessed 12 January 2021.

ANVISA, 2020. "ResoluÇÃo - rdc nº 356, de 23 de marÇo de 2020, publicada no dou em 23/03/2020". *Órgão: Ministério da Saúde/Agência Nacional de Vigilância Sanitária.*, Vol. 26, No. 1C, pp. 1–5.

Callister, W.D.J., 2000. *Ciência e Engenharia de Materiais: Uma introdução*. LTC, Rio de Janeiro.

Dao, K. and Dicken, D., 1987. "Fatigue failure mechanisms in polymers". Wiley Online Library, https://onlinelibrary.wiley.com/doi/abs/10.1002/pen.760270406. Accessed 13 may 2021.

De Almeida, G.R., 2018. "Cabos aéreos para linhas de transmissão de energia elétrica: Com referências às suas resistências às vibrações eólicas". Cabos para transmissão de energia, https://www.osetoreletrico.com.br/cabos-para-transmissao-de-energia/. Accessed 13 may 2021.

Kalaga, S. and Neelam, M.K., 2002. "Elastic properties of pvc pipes". www.researchgate.net/publication/281786040/ElasticpropertiesofPVCpipes. Accessed 13 May 2021.

MatWeb, 2021. "Aluminum 1350-h19". http://www.matweb.com/search/DataSheet. Accessed 13 may 2021.

Mohammadian, M., Choobineh, A., Haghdoost, A. and Hasheminejad, N., 2014. "Normative data of grip and pinch strengths in healthy adults of iranian population". Iranian Journal of Public Health, https://www.ncbi.nlm.nih.gov/pmc/articles/PMC4411908/. Accessed 13 may 2021.

NIOSH, 2015. "Workplace solutions: preparedness through daily practice: the myths of respiratory protection in healthcare publication no. 2016-109. cincinnati, oh: U.s. department of health and human services, centers for disease control and prevention, national institute for occupational safety and health, dhhs (niosh); 2015." *National Institute for Occupational Safety and Health.*

Petyt, M., 2010. *Introduction to Finite Element Vibration Analysis*. Cambridge University Press.

Rosa, M., Chaves, G., Alaves, M. and Machado, M., 2020. *PESQUISA TRANSLACIONAL EM SAÚDE PARA O ENFRENTAMENTO DO COVID-19: desenvolvimento e produção do respirador VESTA como equipamento de proteção individual. In: Aldira Guimarães Duarte; Carlos F. Domínguez Avila. (Org.). A COVID-19 NO BRASIL: ciência, inovação tecnológica e políticas públicas.* Editora CRV.

Shereen, M.A., S.Khan, A.Kazmi, Bashir, N. and Siddique, R., 2020. "Covid-19 infection: Origin, transmission, and characteristics of human coronaviruses." *Journal of Advanced Research*, Vol. 24, pp. 91–98.

Stolarski, T., Nakasone, Y. and Yoshimoto, S., 2006. *Engineering Analysis with ANSYS Software*. Elsevier Butterworth-Heinemann, 1st edition. ISBN 075066875X.

Thomas, S., Joseph, K., Malhotra, S.K., Goda, K. and Sreekala, M.S., 2012. "Advances in polymer composites: Macro- and microcomposites— state of the art, new challenges, and opportunities". *Polymer Composites*, Vol. 1, No. 1, pp. 1–16.

Zhipeng, L. and James, Y., 2013. "Computer-aided customized shape design of an n95 filtering facepiece respirator". In *Proceedings of the ASME 2013 International Design Engineering Technical Conferences and Computers and Information in Engineering Conference IDETC/CIE 2013*. Portland, Oregon, USA.

Zhipeng, L., Yang, J. and Zhuang, Z., 2012. "Headform and n95 filtering facepiece respirator interaction: Contact pressure simulation and validation." *Journal of Occupational and Environmental Hygiene*, Vol. 9, No. 1, p. 46–58.

9. RESPONSIBILITY NOTICE

The following text, properly adapted to the number of authors, must be included in the last section of the paper:
The author(s) is (are) solely responsible for the printed material included in this paper.